A Comparative Investigation of Benzo[*a*]pyrene, Procaine and Nevirapine Metabolism in Human Hepatocytes and a 3D Skin Tissue Model

Joanna E. Barbara, Emily Sibala, Seema Muranjan, Forrest Stanley, and David B. Buckley

XenoTech LLC, 1101 W Cambridge Circle Drive, Kansas City, Kansas 66103 USA

Introduction

Skin metabolism is an important contributor to the safety and efficacy of dermally applied drugs, despite the fact that drug metabolizing enzyme activity is typically lower in the skin than in other organs more commonly associated with metabolism (Oesch *et al.*, 2007). Therefore *in vitro* skin metabolism assays are necessary for development of topically-applied compounds. Knowledge of the drug metabolizing enzymes present in skin is incomplete, but several cytochrome P450 enzymes, flavin-dependent monooxygenases, alcohol and aldehyde dehydrogenases, various hydrolytic enzymes, and conjugation enzymes including glutathione *S*-transferase, glucuronosyltransferase, sulfotransferase, acetyltransferases and methyl transferase have been characterized in mammalian skin (Oesch *et al.*, 2007; van Eijl *et al.*, 2012). Consequently, skin metabolism can be as diverse as liver metabolism and needs careful experimentation to fully understand exposure profiles. The European animal testing ban of 2013 recently further reinforced the need for simple and reliable skin metabolism modeling assays for cosmetics safety testing. Procuring and working with skin-based test systems can be challenging. Viable whole skin for short-term culture is difficult to obtain and expensive apparatus are needed. Skin has high collagen content, which makes it difficult to process to subcellular fractions. Drug metabolizing enzymes found in skin are generally localized to keratinocytes in the epidermis making them a viable option, but they are difficult to isolate and culture, and culture conditions can strongly affect the drug metabolizing capabilities of the cells (Oesch, *et al.*, 2007). The use of normal human 3D skin tissue models for genotoxicity and sensitization assays is rapidly increasing as an alternative approach (Brinkmann *et al.*, 2013). In the present study, the commercially-available 3D skin model EpiDerm™ (MatTek, Ashland, MA) was evaluated for metabolism of the three diverse test compounds benzo[*a*]pyrene, procaine and nevirapine and was compared to the well-established liver metabolism model cryopreserved human hepatocytes. EpiDerm™ is a tissue culture model comprising reconstructed human epidermal cells differentiated into keratinocytes, resulting in a close representation of the human epidermis (Boelsma *et al.*, 2000).

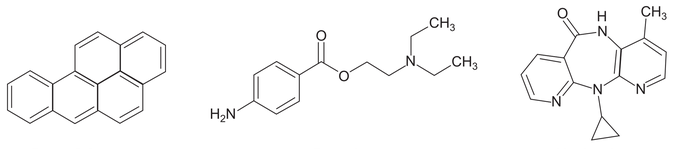

Benzo[*a*]pyrene **Procaine** **Nevirapine**

Materials & Methods

The EpiDerm™ samples were conditioned overnight in medium at 37°C for acclimation and were then exposed to the test drugs by deposition of a 30 µL aliquot of 1 mM drug in acetone (benzo[*a*]pyrene and nevirapine) or water (procaine) to yield a 50 nmol/cm^2 concentration. At 0, 24 and 48 h, incubations were stopped by extraction of the tissue layer which was immediately frozen at −80°C. The keratinocyte layer was homogenized with 1xPBS buffer at 1:8 w/v. Aliquots were treated with an equal volume of acetonitrile for protein precipitation. Cryopreserved human hepatocytes (1 million cells/mL) were incubated with 10 µM drug for up to 4 h and were prepared by protein precipitation with acetonitrile. Samples were analyzed for metabolite profiling with UHPLC methods with a Waters Acquity LC system coupled to a Waters Xevo G2-XS quadrupole time of flight accurate mass spectrometer. The mass spectrometer was operated in positive or negative resolution elevated energy mass spectrometry (MS^E) or MSMS mode with electrospray ionization. Metabolites were separated on a Waters BEH C18 column (1.7 µm, 2.1 x 100 mm) with 0.1% formic acid in water or acetonitrile (0.4 mL/min) using compound-specific gradient methods. Fexofenadine was employed for real-time mass calibration. Data processing employed MetaboLynx XS and QuanLynx subroutines of Waters MassLynx version 4.1 (Milford, MA) and metabolite structural elucidation was performed manually.

Results

Benzo[*a*]pyrene was metabolized by both the human skin model and the human hepatocytes. Thirteen oxidized metabolites of benzo[*a*]pyrene (B1 through B13) were observed overall (**Table 1**), consistent with the known extensive oxidation and conjugation of benzo[*a*]pyrene and other polyaromatic hydrocarbons in humans. All of the metabolites were detected with better than 10 ppm mass accuracy. The observed metabolites were consistent with epoxidation allowed by epoxide hydrolysis to yield the dihydrodiol through the tetraol, and hydroxylation, with and without glucuronide and sulfate conjugation. No glutathione-conjugated metabolites were observed in either test system. Only two metabolites were detected in the hepatocyte incubation samples (**Figure 1**). These comprised a mono-oxidation metabolite and a glucuronide-conjugated oxygenated metabolite. All thirteen metabolites were detected in the EpiDerm™ incubations (**Figure 2**), demonstrating that oxidative metabolism, epoxide hydrolysis, and glucuronide and sulfate conjugation were all supported by the skin model test system. Observation of oxidative metabolism of benzo[*a*]pyrene in the skin model was consistent with the findings of Brinkmann *et al.* (2012), but minimal information on conjugation metabolism in EpiDerm™ incubations is available for comparison. As expected, metabolism of benzo[*a*]pyrene was more extensive in the skin model than in the suspended hepatocytes (**Figure 3**).

Table 1. Metabolite profile for benzo[*a*]pyrene incubated at 10 µM for up to 4 h with human hepatocytes (1 million cells/mL) and at 50 nmol/cm^2 for up to 48 h with the EpiDerm™ model

Component	Retention time (min)	Experimental *m/z*	Theoretical *m/z*	Mass error (ppm)	Mass shift	Elemental composition	Proposed biotransformation	Hepatocytes			EpiDerm™	
								1 Hr	2 Hr	4 Hr	24Hr	48 Hr
B1	2.32	319.0959	319.0970	3.4	+68.0098	$C_{20}H_{16}O_4$	Poly-oxidation	ND	ND	ND	✔	✔
B2	2.62	363.0293	363.0327	9.4	+111.9432	$C_{20}H_{12}O_5S$	Di-oxidation + sulfation	ND	ND	ND	✔	✔
B3	3.53	635.1429	635.1400	4.6	+384.0568	$C_{32}H_{28}O_{14}$	Di-oxidation + di-glucuronidation	ND	ND	ND	ND	✔
B4	4.28	301.0875	301.0865	3.3	+50.0014	$C_{20}H_{14}O_3$	Di-oxidation + epoxidation	ND	ND	ND	✔	✔
B5	4.77	459.1067	459.1080	2.8	+208.0026	$C_{26}H_{20}O_8$	Di-oxidation + glucuronidation	ND	ND	ND	✔	✔
B6	4.81	319.0959	319.0970	-3.4	+68.0098	$C_{20}H_{14}O_3$	Poly-oxidation	ND	ND	ND	ND	✔
B7	5.13	319.0959	319.0970	-3.4	+68.0098	$C_{20}H_{16}O_4$	Poly-oxidation	ND	ND	ND	✔	✔
B8	5.33	635.1407	635.1400	1.1	+384.0726	$C_{32}H_{28}O_{14}$	Di-oxidation + di-glucuronidation	ND	ND	ND	✔	✔
Benzo[*a*]pyrene	5.72	251.0941	251.0861	31.9	+0.0080	$C_{20}H_{12}$	Not applicable	✔	✔	✔	✔	✔
B9	6.35	267.0821	267.0810	4.1	+15.9949	$C_{20}H_{12}O$	Mono-oxidation	ND	ND	ND	✔	✔
B10	6.50	459.1087	459.1080	1.5	+208.0406	$C_{26}H_{20}O_8$	Di-oxidation + glucuronidation	ND	ND	ND	✔	✔
B11	6.52	443.1130	443.1131	0.2	+192.0269	$C_{26}H_{20}O_7$	Mono-oxidation + glucuronidation	✔	✔	✔	✔	✔
B12	7.62	267.0811	267.0810	0.4	+15.9950	$C_{20}H_{12}O$	Mono-oxidation	✔	✔	✔	✔	✔
B13	8.37	267.0814	267.0810	1.5	+15.9953	$C_{20}H_{12}O$	Mono-oxidation	ND	ND	ND	✔	✔

ND: Not detected ✔ *Detected*

Figure 1. Extracted accurate mass ion chromatograms showing benzo[*a*]pyrene and metabolites detected after incubation of 10 µM benzo[*a*]pyrene with human hepatocytes (1 million cells/mL) for 4 h

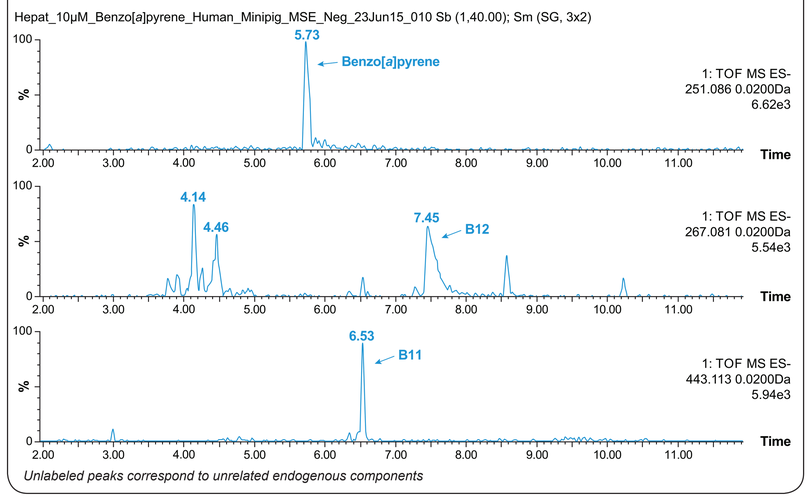

Unlabeled peaks correspond to unrelated endogenous components

Figure 2. Extracted accurate mass ion chromatograms showing benzo[*a*]pyrene and metabolites detected after incubation of 50 nmol/cm^2 benzo[*a*]pyrene with the EpiDerm™ skin model for 48 h

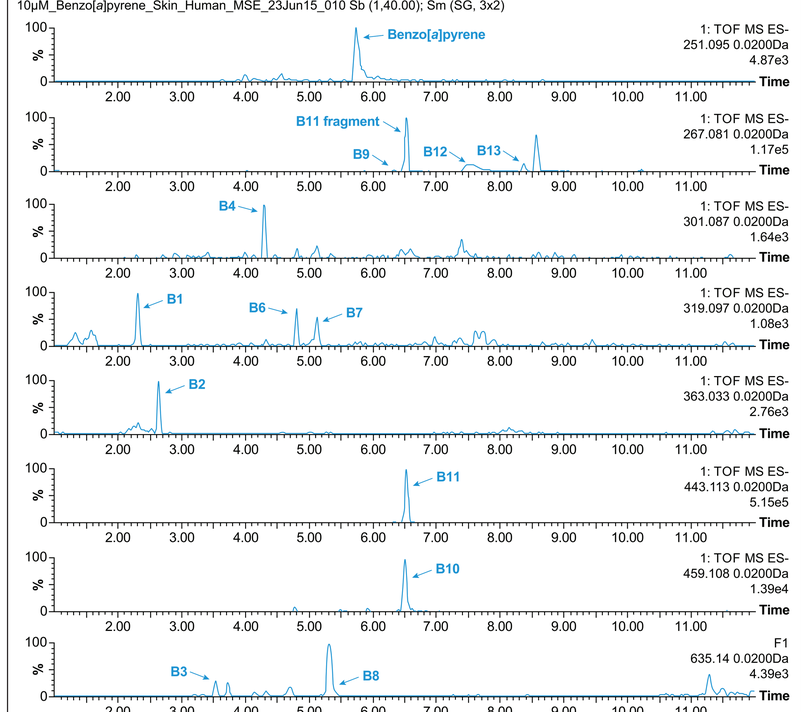

Unlabeled peaks correspond to unrelated endogenous components

Figure 3. Comparative metabolism of benzo[*a*]pyrene incubated at 10 µM for up to 4 h with human hepatocytes (1 million cells/mL) and at 50 nmol/cm^2 for up to 48 h with the EpiDerm™ skin model

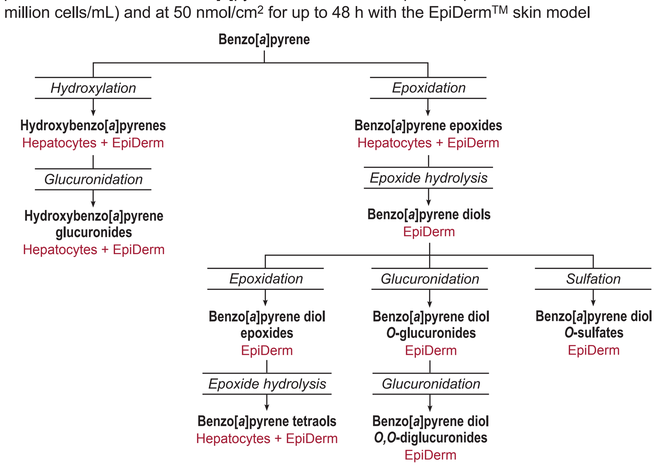

Procaine was also metabolized by both the skin model and the human hepatocytes (**Table 2**; **Figure 4**). The primary route of procaine metabolism *in vivo* is through carboxylesterase-mediated ester hydrolysis to yield *p*-aminobenzoic acid (Jewell *et al.*, 2007). The *p*-aminobenzoic metabolite was observed in both hepatocyte and skin model incubations, indicating that carboxylesterase activity is supported by the EpiDerm™ model as well as by hepatocytes. The corresponding hydrolysis product diethylaminoethanol was not observed in either test system. The secondary metabolite formed by N-acetylation of *p*-aminobenzoic acid, *N*-acetylamidobenzoic acid, was also observed in both test systems, demonstrating the EpiDerm™ model as capable of supporting *N*-acetyltransferase-mediated metabolism. This was consistent with the observation of direct N-acetylation of procaine observed in both hepatocyte and skin model incubations. However, none of the known *in vivo* glucuronide or glycine conjugates were detected in either test system. The overall extent of procaine metabolism in the skin model was similar to the extent of metabolism observed in the human hepatocytes.

Table 2. Metabolite profile for procaine incubated at 10 µM for up to 4 h with human hepatocytes (1 million cells/mL) and at 50 nmol/cm^2 for up to 48 h with the EpiDerm™ model

Component	Retention time (min)	Experimental *m/z*	Theoretical *m/z*	Mass error (ppm)	Mass shift	Elemental composition	Proposed biotransformation	Hepatocytes			EpiDerm™	
								1 Hr	2 Hr	4 Hr	24Hr	48 Hr
p-Aminobenzoic acid	2.19	138.0553	138.0555	-1.4	-99.1050	$C_7H_7NO_2$	Ester hydrolysis	✔	✔	✔	✔	ND
Procaine	3.50	237.1609	237.1603	-2.5	+0.0006	$C_{13}H_{20}N_2O_2$	Not applicable	✔	✔	✔	✔	✔
N-Acetylamido benzoic acid	5.56	180.0663	180.0661	1.1	-57.0940	$C_9H_9NO_3$	Ester hydrolysis + N-acetylation	✔	✔	✔	✔	✔
N-Acetylprocaine	5.82	279.1709	279.1709	0	+42.0106	$C_{15}H_{22}N_2O_3$	Ester hydrolysis + N-acetylation	✔	✔	✔	✔	✔

ND: Not detected ✔ *Detected*

Nevirapine was only metabolized by the human hepatocytes (**Table 3**; **Figure 5**). Nevirapine substrate loss in the hepatocyte incubations was minimal, but four nevirapine metabolites (N1 through N4) were observed. Three of the metabolites (N1 through N3) were formed by nevirapine hydroxylation. Metabolite N1 was a glucuronide conjugate of hydroxynevirapine, but there was no evidence of the expected corresponding sulfate conjugate. Nevirapine substrate loss was observed in the skin model incubations, but no metabolites were detected. These results are consistent with low hydroxynevirapine formation and the extensive covalent binding known to be associated with nevirapine metabolites (Sharma *et al.*, 2013).

Table 3. Metabolite profile for nevirapine incubated at 10 µM for up to 4 h with human hepatocytes (1 million cells/mL) and at 50 nmol/cm^2 for up to 48 h with the EpiDerm™ model

Component	Retention time (min)	Experimental *m/z*	Theoretical *m/z*	Mass error (ppm)	Mass shift	Elemental composition	Proposed biotransformation	Hepatocytes			EpiDerm™	
								1 Hr	2 Hr	4 Hr	24Hr	48 Hr
N1	4.67	459.1522	459.1516	1.3	+192.0276	$C_{21}H_{22}N_4O_8$	Hydroxylation + glucuronidation	ND	✔	✔	ND	ND
N2	5.48	283.1193	283.1195	0.7	+15.9949	$C_{15}H_{14}N_4O_2$	Hydroxylation	✔	✔	✔	ND	ND
N3	5.61	283.1197	283.1195	-0.7	+15.9949	$C_{15}H_{14}N_4O_2$	Hydroxylation	✔	✔	✔	ND	ND
N4	5.72	227.0919	227.0933	-6.2	-40.0327	$C_{12}H_{10}N_4O_2$	N-dealkylation	✔	✔	✔	ND	ND
Nevirapine	6.49	267.1252	267.1246	-2.3	+0.0006	$C_{15}H_{14}N_4O$	–	✔	✔	✔	✔	✔

ND: Not detected ✔ *Detected*

Figure 4. Comparative metabolism of procaine incubated at 10 µM for up to 4 h with human hepatocytes (1 million cells/mL), at 50 nmol/cm^2 for up to 48 h with the EpiDerm™ skin model

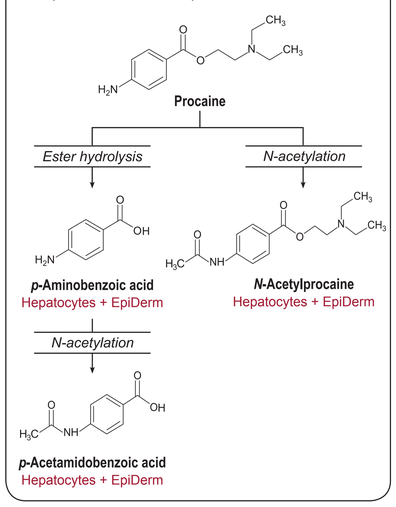

Figure 5. Metabolism of nevirapine incubated at 10 µM for up to 4 h with human hepatocytes (1 million cells/mL)

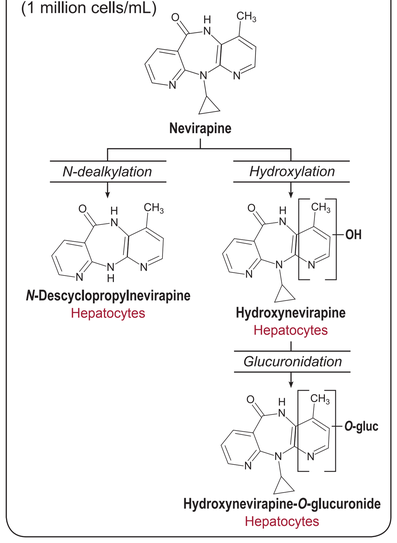

Conclusions

- In conclusion, allowing for differences in expression of drug metabolizing enzymes across tissues, the metabolite profiles derived for the skin model were comparable to those determined for the human hepatocytes for two out of three of the test drugs.
- The EpiDerm™ model was demonstrated as a promising tool for evaluating skin metabolism of some dermally-applied compounds in that metabolites produced by diverse-range test systems were observed.
- The EpiDerm™ model produced oxidized, reduced, hydrolyzed and conjugated (glucuronide, sulfonate and *N*-acetyl metabolites).
- Further characterization work is necessary to establish when the EpiDerm™ model may be a suitable system for *in vitro* skin metabolism studies.

References

1. Boelsma E, Gibbs S, Faller C and Ponec M (2000) Characterization and comparison of reconstructed skin models: Morphological and immunohistochemical evaluation. *Acta Derm Venereol* **80:** 82-88.
2. Brinkmann J, Stolpmann K, Trappe S, Otter T, Genkinger D, Bock U, Liebsch M, Henkler F, Hutzler C and Luch A (2013) Metabolically competent human skin models: Activation and genotoxicity of benzo[*a*]pyrene. *Toxicol Sci* **131(2):** 351-359.
3. Jewell C, Ackermann C, Payne NA, Fate G, Voorman R and Williams FM (2007) Specificity of procaine and ester hydrolysis by human, minipig, and rat skin and liver. *Drug Metab Dispos* **35:** 2015-2022.
4. Oesch F, Fabian E, Oesch-Bartlomowicz B, Werner C and Landsiedel R (2007) Drug-metabolizing enzymes in the skin of man, rat and pig. *Drug Metab Rev* **39:** 659-698.
5. Sharma AM, Klarskov K and Uetrecht J (2013) Nevirapine bioactivation and covalent binding in the skin. *Chem Res Toxicol* **26:** 410-421.
6. Trushin N, Alam S, El-Bayoumy K, Krzeminski J, Amin S, Gullett J, Meyers C and Prokopczyk B (2012) Comparative metabolism of benzo[*a*]pyrene by human keratinocytes infected with high-risk human papillomavirus types 16 and 18 as episomal or integrated genomes. *J Carcinog* **11:** 1.
7. van Eijl S, Zhu Z, Cupitt J, Gierula M, Götz C, Fritsche E and Edwards RJ (2012) Elucidation of xenobiotic metabolism pathways in human skin and human skin models by proteomic profiling. *PLOS One* 2012:7; e41721.